

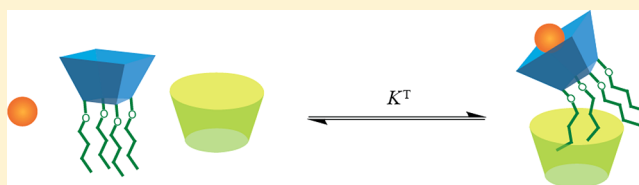
# Independent Pathway Formation of Guest–Host in Host Ternary Complexes Made of Ammonium Salt, Calixarene, and Cyclodextrin

Nuno Basílio, Vitor Francisco, and Luis García-Río\*

Departamento Química Física, Centro Singular de Investigación en Química Biológica y Materiales Moleculares (CIQUS), Universidad de Santiago, 15782 Santiago, Spain

**S** Supporting Information

**ABSTRACT:** The interaction between  $\gamma$ -cyclodextrin and amphiphilic *p*-sulfonatocalix[4]arenes was studied using NMR and isothermal titration calorimetry techniques. The results indicate that these calixarenes are able to form 1:1, 1:2, and 2:1 host–guest complexes with the cyclodextrin. The ROESY spectra suggest that the cyclodextrin binds the calixarenes through the hydrophobic alkyl chains. *p*-Sulfonatocalix[4]arenes, which are traditionally used as host molecules, act as guests in the presence of  $\gamma$ -cyclodextrin. However, their recognition site remains active upon complexation with the cyclodextrin, and ternary complexes can be devised. Here, we also demonstrate the formation of such complexes using tetramethylammonium chloride as a model guest. Moreover, it is also demonstrated that the recognition properties of the calixarene are unaffected upon complexation with the cyclodextrin.



## INTRODUCTION

Macrocyclic compounds such as cyclodextrins,<sup>1</sup> calixarenes,<sup>2</sup> cucurbiturils,<sup>3</sup> and cavitands<sup>4</sup> are well-known host molecules, frequently designated as molecular containers because of their ability to completely or partially include guest species in their cavities. Fundamental research on these systems is of great significance because the molecular behavior of guest molecules included within the nanocavity of these macrocyclic hosts can be related to that of molecules inside biochemical structures and significantly different from that observed in dilute solution.<sup>5</sup> It had been shown that the acidity/basicity,<sup>6,7</sup> reactivity,<sup>8,9</sup> conformation,<sup>10,11</sup> or fluorescence<sup>12</sup> of guest species can be modified upon cavity inclusion.

Of particular interest is the application of molecular encapsulation to control and modulate the ability of guest molecules to self-aggregate.<sup>13–15</sup> The formation of inclusion complexes between cyclodextrins and surfactants is, by far, the most thoroughly studied system in this field.<sup>13</sup> The presence of cyclodextrins in a solution containing surfactant micelles introduces a new equilibrium in the system that, in most cases, displaces the aggregation equilibrium back toward the free monomers. In practice, this means that cyclodextrins shift the critical micelle concentration to higher values and, thus, can be used to disrupt the micellar aggregates.<sup>16–18</sup>

Given the well-known affinity of cyclodextrins to form host–guest complexes with surfactants,<sup>13</sup> we predicted that amphiphilic *p*-sulfonatocalix[*n*]arenes should act as guests in the presence of cyclodextrins. In fact, the formation of such complexes was already reported.<sup>19</sup> Michels et al. found that amphiphilic calix[4]arene carboxylate derivatives bearing two lower rim attached propoxyphenyl groups or four tetrapropoxy groups form 1:1 complexes with  $\gamma$ -CD. However, the formation of ternary complexes between cyclodextrin, calixarenes, and

other small molecules or ions remains unexplored. One of the objectives of this work was to check if the recognition properties of the calixarene are affected when a remote segment of this molecule (i.e., the alkyl chains) is complexed by the cyclodextrin.

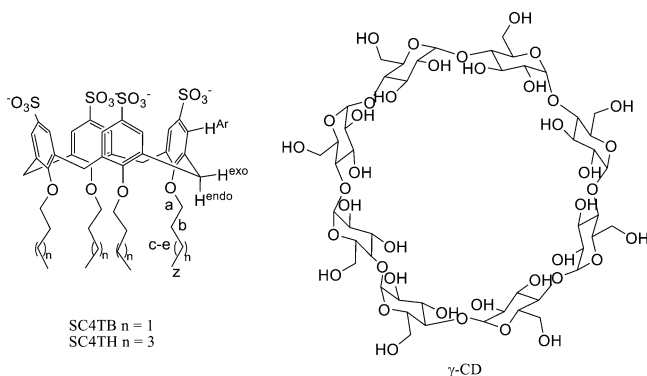
Conversely, we decided to study the formation of ternary complexes between cyclodextrin, calixarenes, and other small molecules or ions and compare their stability with the correspondent binary complexes. The formation of complexes between two or more macrocycles and small guest molecules is relatively rare, though some examples can be found in the literature. For example, the inclusion of metal cation–crown ether complexes inside dimeric capsules made of *p*-sulfonatocalixarenes had been reported.<sup>20</sup> Cucurbiturils were also applied in this field;<sup>21–23</sup> the example of the inclusion of cationic calix[4]arene inside the cavity of cucurbit[10]uril<sup>22</sup> was quite remarkable due to the observed positive allostereism.

In the present work, the interaction of  $\gamma$ -CD with amphiphilic *O*-alkylated *p*-sulfonatocalix[4]arenes (Scheme 1) was investigated by NMR and microcalorimetric techniques. *p*-Sulfonatocalix[*n*]arenes are also known to form host–guest complexes with a variety of molecules and ions.<sup>24</sup> Thus, besides studying the interaction of *O*-alkylated *p*-sulfonatocalix[4]arenes with  $\gamma$ -CD, the interaction of a model guest, tetramethylammonium chloride (TMA), with the calix[4]arene derivative and the formation of ternary complexes (between the cyclodextrin, the calix[4]arene and TMA) was also investigated.

Received: September 27, 2012

Published: November 8, 2012

Scheme 1



## RESULTS AND DISCUSSION

**Complex Stoichiometry.** The interaction of tetrasodium 5,11,17,23-tetrasulfonato-25,26,27,28-tetrakis(*n*-butyl)calix[4]arene (SC4TB) and tetrasodium 5,11,17,23-tetrasulfonato-25,26,27,28-tetrakis(*n*-hexyl)calix[4]arene (SC4TH) with  $\gamma$ -CD was first probed by isothermal titration calorimetry (ITC). Both SC4TB and SC4TH are blocked into the cone conformation, and it is known that these calix[4]arenes self-assemble into micellar aggregates in aqueous solution.<sup>25–28</sup> In order to avoid any interference of the self-aggregation process in the titration experiments, it is convenient to carry out the measurements below the critical micelle concentration (cmc) of SC4TB (3.2 in H<sub>2</sub>O and 2.3 mM in D<sub>2</sub>O) and SC4TH (0.49 in H<sub>2</sub>O and 0.32 mM in D<sub>2</sub>O).<sup>25,28</sup> The measurements were performed by titrating a stock solution of  $\gamma$ -CD into the calorimetric cell containing a solution with a known concentration of SC4TH or SC4TB. The resulting enthalpograms and titration curves (integrated heat changes per mole of

injectant versus  $[\gamma\text{-CD}]/[\text{surfactant}]$  molar ratio) are shown in Figure 1.

The nonlinear fit of the titration data to a 1:1 binding model gives a line that deviates considerably from the experimental data (see Figure S1, Supporting Information). This strongly suggests that, within the experimental conditions, higher stoichiometry complexes are present in solution. On the other hand, if 1:1 and 1:2 cyclodextrin/calixarene complexes are considered, the theoretical model (two sequential binding sites) can be properly fitted to the experimental data (see Figure 1). Though these results support the formation of such type of complexes, it is desirable to obtain further information by other techniques.

To complement the microcalorimetric experiments, we have employed <sup>1</sup>H NMR techniques to study the complexation of amphiphilic calixarenes by  $\gamma$ -CD. <sup>1</sup>H NMR titration experiments along with the Job's method were used to evaluate the stability and stoichiometry of the complexes. As an example, Figure 2 shows the data obtained for the *c* (see Scheme 1) protons of SC4TB. All other <sup>1</sup>H NMR signals present similar downfield or upfield displacements upon addition of  $\gamma$ -CD (see the Supporting Information). The changes observed in the <sup>1</sup>H NMR spectra can be attributed to the formation of an inclusion complex between the SC4TB and the cyclodextrin. More specifically, the  $\delta_{\text{obs}}$  displacement can be caused by a change in the microenvironment experienced by the guest upon inclusion.<sup>19</sup>

As can be observed in Figure 2, the maximum in the Job's plot is observed when the mole fraction ( $[\gamma\text{-CD}]/([\text{SC4TB}] + [\gamma\text{-CD}])$ ) is approximately 0.4. When 1:2 complexes are present in solution the maximum is expected at 0.33, and when only 1:1 complexes are formed the maximum value appears at 0.5. The value observed for the present case indicates that at least two

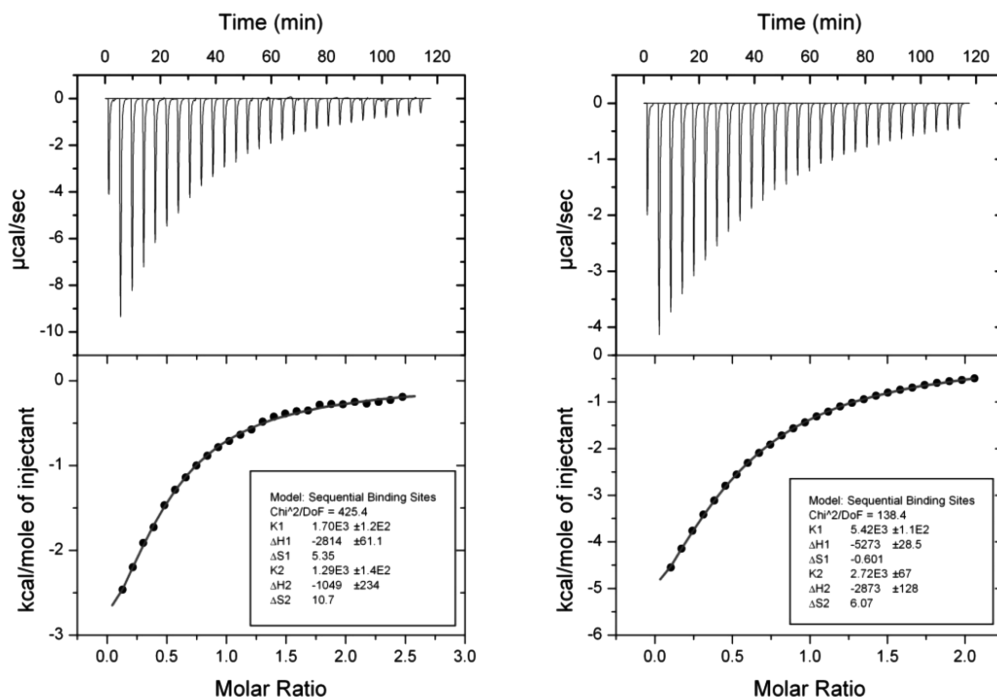


**Figure 1.** Microcalorimetric titration of  $\gamma$ -CD into a solution of SC4TB (left) and SC4TH (right) at 25 °C. The upper part of the graph corresponds to the raw data for 28 sequential injections (10  $\mu$ L per injection) of  $\gamma$ -CD solution (12.5 or 3.0 mM) injecting into a SC4TB (1 mM) or SC4TH solution (0.3 mM). The lower part of the graphs shows the apparent reaction heat obtained from the integration of calorimetric traces.

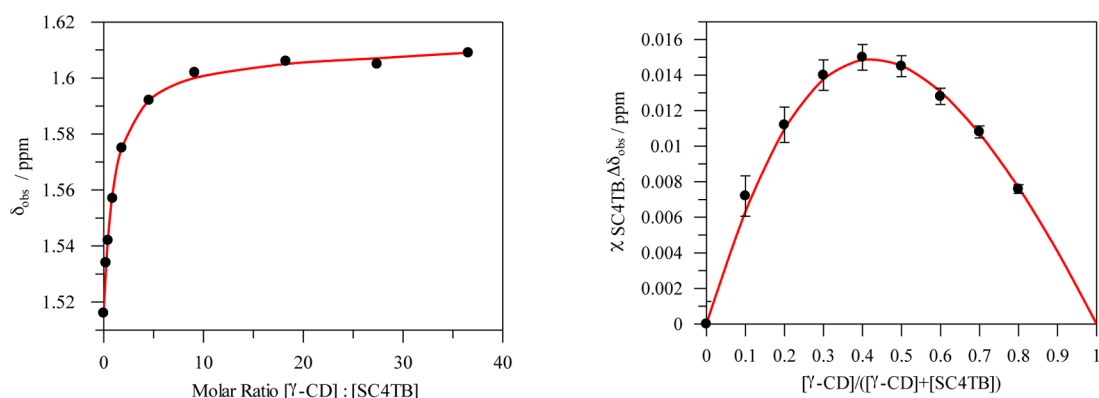


**Figure 2.** (Left) Observed  $^1\text{H}$  NMR chemical shifts ( $\delta_{\text{obs}}$ ) for the  $c$  protons of SC4TB represented against the molar ratio. The concentration of SC4TB was maintained throughout the titration (1 mM). (Right) Job's plot (constructed using the  $c$  protons) for the SC4TB- $\gamma$ -CD complex obtained for a total concentration ( $[\text{SC4TB}] + [\gamma\text{-CD}]$ ) of 1 mM. All  $^1\text{H}$  NMR experiments were carried out at 25  $^\circ\text{C}$  in  $\text{D}_2\text{O}$ . The solid red lines were obtained by fixing  $K_1 = 1700 \text{ M}^{-1}$  and  $K_2 = 1290 \text{ M}^{-1}$  and optimizing the chemical shifts of the  $c$  protons in the 1:1 and 1:2 complexes ( $\delta_{1:1}$  and  $\delta_{1:2}$ ). (Left)  $\delta_{1:1} = 0.096 \text{ ppm}$  and  $\delta_{1:2} = 0.045 \text{ ppm}$  and (right)  $\delta_{1:1} = 0.069 \text{ ppm}$  and  $\delta_{1:2} = 0.052 \text{ ppm}$ .

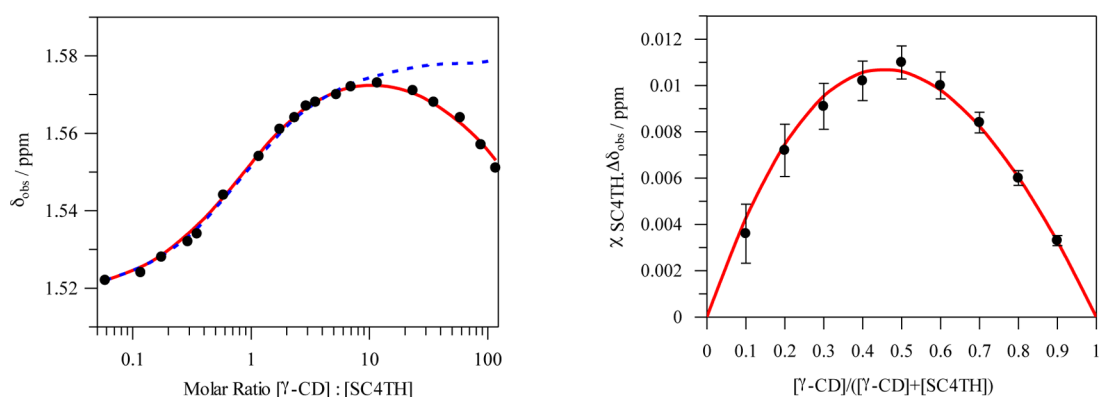
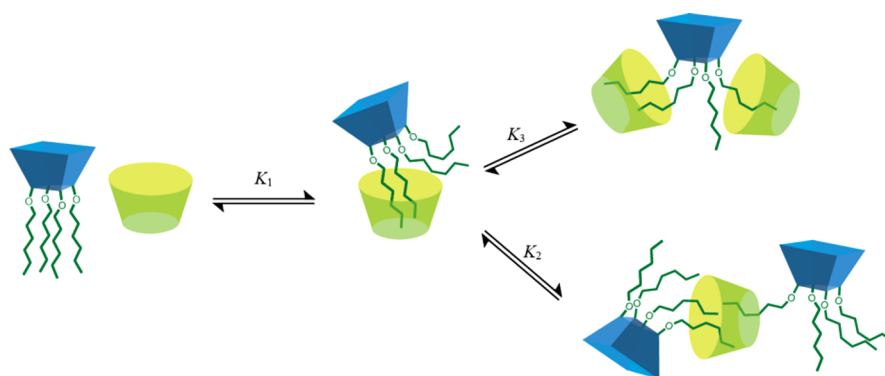


**Figure 3.** (Left) Observed  $^1\text{H}$  NMR chemical shifts ( $\delta_{\text{obs}}$ ) for the  $c$  protons of SC4TH represented against the molar ratio. The concentration of SC4TH was maintained constant throughout the titration (0.29 mM). (Right) Job's plot (constructed using the  $c$  protons) for the SC4TH- $\gamma$ -CD complex obtained for a total concentration ( $[\text{SC4TH}] + [\gamma\text{-CD}]$ ) of 0.23 mM. All  $^1\text{H}$  NMR experiments were carried out at 25  $^\circ\text{C}$  in  $\text{D}_2\text{O}$ . The solid red lines were obtained by fixing  $K_1 = 5420 \text{ M}^{-1}$  and  $K_2 = 2720 \text{ M}^{-1}$  and optimizing  $K_3$  and the chemical shifts of the  $c$  protons in the 1:1, 1:2 and 2:1 complexes ( $\delta_{1:1}$ ,  $\delta_{1:2}$ ,  $\delta_{2:1}$ ). (Left)  $K_3 = 20 \text{ M}^{-1}$ ,  $\delta_{1:1} = 0.061 \text{ ppm}$ ,  $\delta_{1:2} = 0.052 \text{ ppm}$  and  $\delta_{2:1} = -0.006 \text{ ppm}$  and (right)  $K_3 = 20 \text{ M}^{-1}$ ,  $\delta_{1:1} = 0.063 \text{ ppm}$ ,  $\delta_{1:2} = 0.042 \text{ ppm}$  and  $\delta_{2:1} = -0.006 \text{ ppm}$ . The dotted blue line was obtained by considering the 1:2 model with  $K_1 = 5420 \text{ M}^{-1}$ ,  $K_2 = 2720 \text{ M}^{-1}$ ,  $\delta_{1:1} = 0.060 \text{ ppm}$  and  $\delta_{1:2} = 0.050 \text{ ppm}$ .

## Scheme 2



types of complexes are present in solution. In fact, it is known that in this situation the Job's method becomes unreliable.<sup>29</sup>

The formation of 1:1 and 1:2 host/guest complexes between  $\gamma$ -CD and SC4TB is also supported by the simulation curves presented in Figure 2. These lines are obtained by applying the mathematical model that considers the formation of both 1:1 and 1:2 complexes (see the Supporting Information for details).

In this model, the binding constants obtained by ITC are kept constant and the chemical shifts of a given NMR signal are optimized for both complexes. As can be observed, the experimental data are well described by the model. The change of chemical shifts associated with the formation of the 1:1 and 1:2 complexes obtained from the titration ( $\Delta\delta_{1:1} = 0.096$ ;  $\Delta\delta_{1:2} = 0.045$ ) and from the Job's method ( $\Delta\delta_{1:1} = 0.069$ ;  $\Delta\delta_{1:2} =$

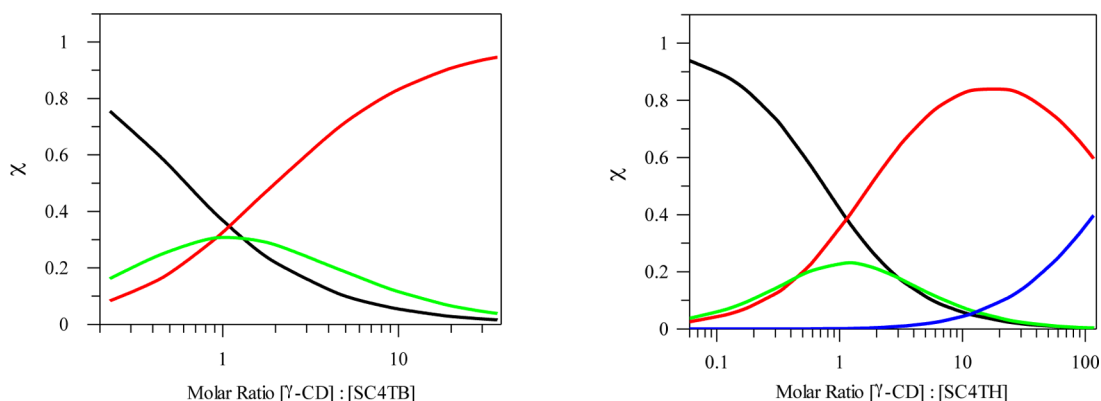


**Figure 4.** Mole fraction ( $\chi$ ) distribution of free calixarene guest (black line), 1:1 complex (red line), 1:2 complex (green line), and 2:1 complex (blue line) represented against the molar ratio. (Left) SC4TB and (right) SC4TH.

0.052) are fairly compatible taking into account the large errors associated with the Job's plot.

The complexation of SC4TH with  $\gamma$ -CD was also studied by  $^1\text{H}$  NMR. It is interesting to note that in this case the Job's plot (Figure 3) shows a maximum value at 0.5 that could be wrongly attributed to the formation of 1:1 binding stoichiometry. However, both the ITC and the  $^1\text{H}$  NMR titration clearly indicate the existence of higher order complexes. Contrary to case of SC4TB, when the 1:2 binding model is applied along with the binding constants obtained by ITC, the experimental behavior cannot be reproduced. However, it is worth noting, that for a molar ratio below 5 the experimental data can be well fitted to the theoretical model (Figure 3). The fact that the experimental data points start to deviate from the 1:2 model for high concentrations of  $\gamma$ -CD is indicative of the formation of 2:1 complexes. Moreover, when the simultaneous formation of 1:1, 1:2, and 2:1 complexes is considered (Scheme 2), both the Job's plot and  $^1\text{H}$  NMR titration can be nicely fitted to the theoretical model (see the details in the Supporting Information). In this case, both  $K_1 = 5420 \text{ M}^{-1}$  and  $K_2 = 2720 \text{ M}^{-1}$  were kept constant, and a value of  $K_3 = 20 \text{ M}^{-1}$  was estimated for the stepwise binding constant correspondent to the formation of 2:1 complexes. Other selected  $^1\text{H}$  NMR signals are also well described by this model (see the Supporting Information). It must be noted that  $K_3$ ,  $\delta_{1:1}$ ,  $\delta_{1:2}$ , and  $\delta_{2:1}$  values are only estimated since it is very difficult to obtain statistically significant values with such a number of fitting parameters.<sup>29</sup> In Figure 4, the mole fraction distribution of the several species, considering the above equilibrium constants, is plotted against the molar ratio used for the  $^1\text{H}$  NMR titrations. It is worth noting that in the ITC conditions the mole fraction of the 2:1 complex is irrelevant, and thus, the microcalorimetric data can be fitted to the simple 1:2 binding model.

DOSY experiments were also performed to further confirm the formation of the calixarene- $\gamma$ -CD complexes. This experiment allows the determination of the diffusion coefficients ( $D$ ) of the species in solution and is particularly useful for studying host-guest systems because both host, guest and complex have their own  $D$  value which is closely related to their shape and molecular weight.<sup>30</sup> Figure 5 shows the influence of the  $\gamma$ -CD concentration on the observed diffusion coefficient ( $D_{\text{obs}}$ ) of SC4TH. As the concentration of  $\gamma$ -CD increases  $D_{\text{obs}}$  decreases due to the association of SC4TH with the  $\gamma$ -CD to form complexes with higher molecular weight than that of the free species. When the exchange between complex

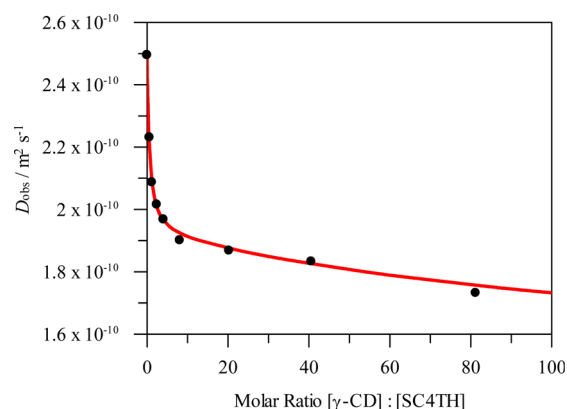


**Figure 5.** Observed diffusion coefficient ( $D_{\text{obs}}$ ) of SC4TH (0.29 mM) represented against the  $[\gamma\text{CD}]/[\text{SC4TH}]$  molar ratio. All experiments were carried out at 25 °C in  $\text{D}_2\text{O}$ . The solid red lines were obtained by fixing  $K_1 = 5420 \text{ M}^{-1}$ ,  $K_2 = 2720 \text{ M}^{-1}$  and  $K_3 = 20 \text{ M}^{-1}$  and optimizing the diffusion coefficients of the 1:1, 1:2 and 2:1 complexes ( $D_{1:1}$ ,  $D_{1:2}$ ,  $D_{2:1}$ ).  $D_{1:1} = 1.91 \times 10^{-6} \text{ cm}^2 \text{ s}^{-1}$ ,  $D_{1:2} = 1.79 \times 10^{-6} \text{ cm}^2 \text{ s}^{-1}$  and  $D_{2:1} = 1.41 \times 10^{-6} \text{ cm}^2 \text{ s}^{-1}$ .

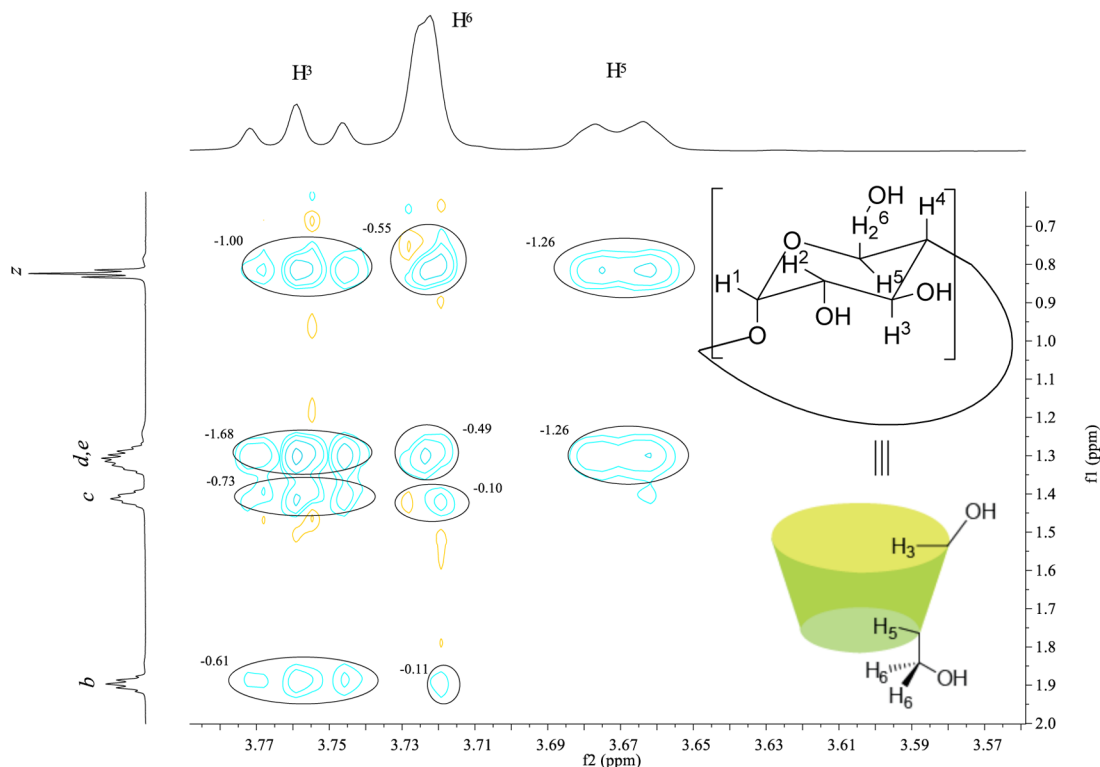
and free species is fast on the NMR time scale, the  $D_{\text{obs}}$  is given by the weighted average of the molecules in the free and complexed states in the same way that the chemical shifts are used. The data presented in Figure 5 was fitted to a global model considering the existence of 1:1, 1:2, and 2:1 species. In the fitting procedure, the binding constants estimated above were kept constant and the diffusion coefficient of the complexes was optimized. As can be observed, the model shows good agreement with the experimental data. From the fitting procedure the following diffusion coefficients were estimated for the 1:1, 1:2, and 2:1 complexes:  $D_{1:1} = 1.91 \times 10^{-6} \text{ cm}^2 \text{ s}^{-1}$ ,  $D_{1:2} = 1.79 \times 10^{-6} \text{ cm}^2 \text{ s}^{-1}$ , and  $D_{2:1} = 1.41 \times 10^{-6} \text{ cm}^2 \text{ s}^{-1}$ , respectively. This tendency follows the expected behavior: the diffusion coefficients decrease as the molecular weight of the complexes increase and, thus, support the proposed model.

**Complex Stability.** From the ITC experiments the values of  $\Delta H^\circ$  and  $\Delta S^\circ$  for the association processes can be directly determined. As already stated, under the conditions of the microcalorimetric experiments the molar fraction of the 2:1 complex is insignificant, so that, in the case of SC4TH, the thermodynamic parameters for the 1:1 and 1:2 obtained by considering two sequential binding sites are not affected by the



**Table 1.** Stepwise Binding Constants ( $M^{-1}$ ) and Thermodynamic Parameters ( $kJ\ mol^{-1}$ ) for the Formation of 1:1 and 1:2  $\gamma$ -Cyclodextrin/Calixarene Complexes Obtained by ITC

|       | $K_1$          | $K_2$          | $\Delta H^\circ_1$ | $\Delta H^\circ_2$ | $T\Delta S^\circ_1$ | $T\Delta S^\circ_2$ |
|-------|----------------|----------------|--------------------|--------------------|---------------------|---------------------|
| SC4TB | $1700 \pm 120$ | $1290 \pm 140$ | $-11.8 \pm 0.3$    | $-4.4 \pm 1.0$     | $6.7 \pm 0.3$       | $13.4 \pm 1.0$      |
| SC4TH | $5420 \pm 110$ | $2720 \pm 67$  | $-22.1 \pm 0.1$    | $-12.0 \pm 0.5$    | $-0.8 \pm 0.1$      | $7.6 \pm 0.5$       |

**Figure 6.** Partial ROESY spectrum of a solution containing 0.5 mM SC4TH and 1 mM  $\gamma$ -CD in  $D_2O$  obtained at 25 °C with a mixing time of 500 ms.

2:1 complex formation. Table 1 summarizes the obtained results for the two calixarenes.

The results shown that the association processes are favored both by enthalpy and entropy, expecting the formation of the 1:1 complex for SC4TH that presents a slightly negative entropy change and that the formation of 1:1 and 1:2 complexes becomes more exothermic when the length of the calixarene alkyl chains increase. On the other hand, the complexation processes become entropically less favorable as the alkyl chain length increases. The fact that  $\Delta H^\circ$  becomes more negative with increasing the alkyl chain length of the guest molecules seems to be a general trend observed in cyclodextrin complexes, but, on the other hand, the variation of  $\Delta S^\circ$  with the alkyl chain length seems to not follow a general trend.<sup>31</sup> The size-fit concept is frequently invoked to explain the thermodynamics trends observed in the formation of cyclodextrin complexes and, in that sense, the fact that  $\alpha$ -CD presents more negative  $\Delta H^\circ$  values for the complexation of straight chain alkanes in comparison with  $\beta$ -CD is generally attributed to the smaller cavity diameter which allows a closer contact between the inner surface of the host and the alkyl chain of the guest, favoring the van der Waals interactions.<sup>31</sup> In addition, the expulsion of water molecules with low coordination number is more efficient in the case of  $\alpha$ -CD, also contributing to make  $\Delta H^\circ$  more negative.<sup>32</sup> In the same way, the interactions established in 1:1 complexes formed from  $\gamma$ -CD and single chain surfactants are usually weaker than for

other cyclodextrins because the alkyl chain is loosely bound inside the cavity.<sup>32–34</sup> In the present case, the enthalpic terms predominates over entropy for the formation of the 1:1 complex suggesting a tight fit of the guest inside the cavity and thus that more than one alkyl chain is included in the cavity of the cyclodextrin.<sup>19</sup> In fact, the incorporation of the two alkyl chains of a gemini surfactant had been proposed previously.<sup>35</sup>

The entropy changes that occur upon complexation are balanced by the release of solvation water molecules both from the cavity of the host and from around the alkyl chains of guest, which contributes to favorable increase in the entropy of system, and by the loss of guest and host rotational and translational degrees of freedom due to conformational changes, that contributes to reduce the entropy of the system.<sup>19,32</sup> In the case studied here the  $\Delta S^\circ$  becomes more unfavorable as the length of the alkyl chains increase suggesting that the loss of degrees of freedom is more important for SC4TH than for SC4TB. Once again, this is commonly observed for guests that fit well the cyclodextrin cavity and are tightly bounded,<sup>19</sup> supporting the suggestion SC4TH is better accommodated inside the host and that more than one alkyl chain is incorporated into the cavity of the  $\gamma$ -CD.

Interpretation of the thermodynamic parameters is more complicated in the case of the 1:2 complexes due to possibility of guest–guest interactions. As the alkyl chain increase similar trends to that observed for 1:1 complexes were found in this

case. However, and in the absence of the complex structure, it is preferable to not speculate on these parameters.

**Complex Structure.** Information about the solution structure of the  $\gamma$ -CD/calixarene complex can be obtained from 2D ROESY experiments. Figure 6 shows part of the ROESY spectra for a solution containing 0.5 mM of SC4TH and 1 mM of  $\gamma$ -CD in D<sub>2</sub>O. Under these conditions, the molar fraction of 2:1 complex is very low (less than 1%) and complex 1:1 dominates (57%). The remaining fraction of SC4TH is present as free guest (16%) and 1:2 complex (26%). The ROESY crosspeak intensity (ROE) is proportional to both the number of equivalent protons and the distance between protons.<sup>36</sup> The observation of ROE crosspeaks between alkyl chain protons of SC4TH and the  $\gamma$ -CD internal protons (H<sup>3</sup>, H<sup>5</sup>, and H<sup>6</sup>) indicates that one or more alkyl chain of the calixarene is incorporated in the cavity of the CD. Moreover, the terminal methyl groups (*z*) of SC4TH alkyl chains interact stronger with the H<sup>5</sup> protons of  $\gamma$ -CD than with H<sup>3</sup>, while the *b* and the *c* protons present more significant ROE with H<sup>3</sup>. These results suggest that, in the predominant 1:1 complex, the calixarene alkyl chains are inserted into the cavity of  $\gamma$ -CD through the wider rim. In the 1:2 it is expected that one calixarene inserts through the wider rim and the second through the opposite tighter rim. In fact, the crosspeak observed for the *b*-H<sup>6</sup> and for the *z*-H<sup>3</sup> proton pairs seems to support this hypothesis.

The ROESY spectrum shows that SC4TH interacts with the  $\gamma$ -CD through the hydrophobic alkyl chains, but however, it does not provide information about the number of alkyl chains that are incorporated inside the cavity of the host.

$\gamma$ -CD is known to form 1:2 host/guest complexes with single chain surfactants. The stability constants for the formation of these species are generally larger than that observed for the formation of 1:1 complexes.<sup>37–39</sup> This indicates that the 1:2 complexes are more stable than the 1:1 complexes and suggests that two alkyl chains are well accommodated inside the  $\gamma$ -CD cavity. The complexation of double chain and gemini surfactants with  $\gamma$ -CD had also been studied and it was demonstrated that the formation of the 1:1 complex is favored over other possible species, and it was suggested that the two alkyl chains are included in the hydrophobic cavity of the  $\gamma$ -CD.<sup>40,41,35</sup>

The noncovalent interactions that stabilize the CD inclusion complexes strongly depend on the space filling of the CD cavity by the guest.<sup>42</sup> Too large or too small guests lead to low binding constants while guests with optimal shape and size lead to more stable complexes. To illustrate some of the possible structures adopted by the 1:1 complex, simple molecular models were built and optimized (SP4 force field) with the Vega-ZZ v.2.4 software.<sup>43</sup> These structures are presented in Figure 7. The models indicate that the four alkyl chains of SC4TH can be simultaneously incorporated in the  $\gamma$ -CD cavity (Figure 7d). However this structure seems unlikely because the four alkyl chains are too voluminous to fit comfortably into the  $\gamma$ -CD cavity. The volume of the  $\gamma$ -CD cavity is approximately 427 Å<sup>3</sup>.<sup>1</sup> Using the methodology proposed by Zhao et al.,<sup>44</sup> a van der Waals volume of 111 Å<sup>3</sup> per hexyl chain was obtained. Considering that the four alkyl chains are fully immersed into the cavity, a packing coefficient (PC) of 1.04 can be calculated. This value is much higher than the optimal 0.55 proposed by Rebek and indicate that this complex should be less stable than the other with less alkyl chains included into the cavity.<sup>45</sup> Though the optimal packing coefficient was originally proposed

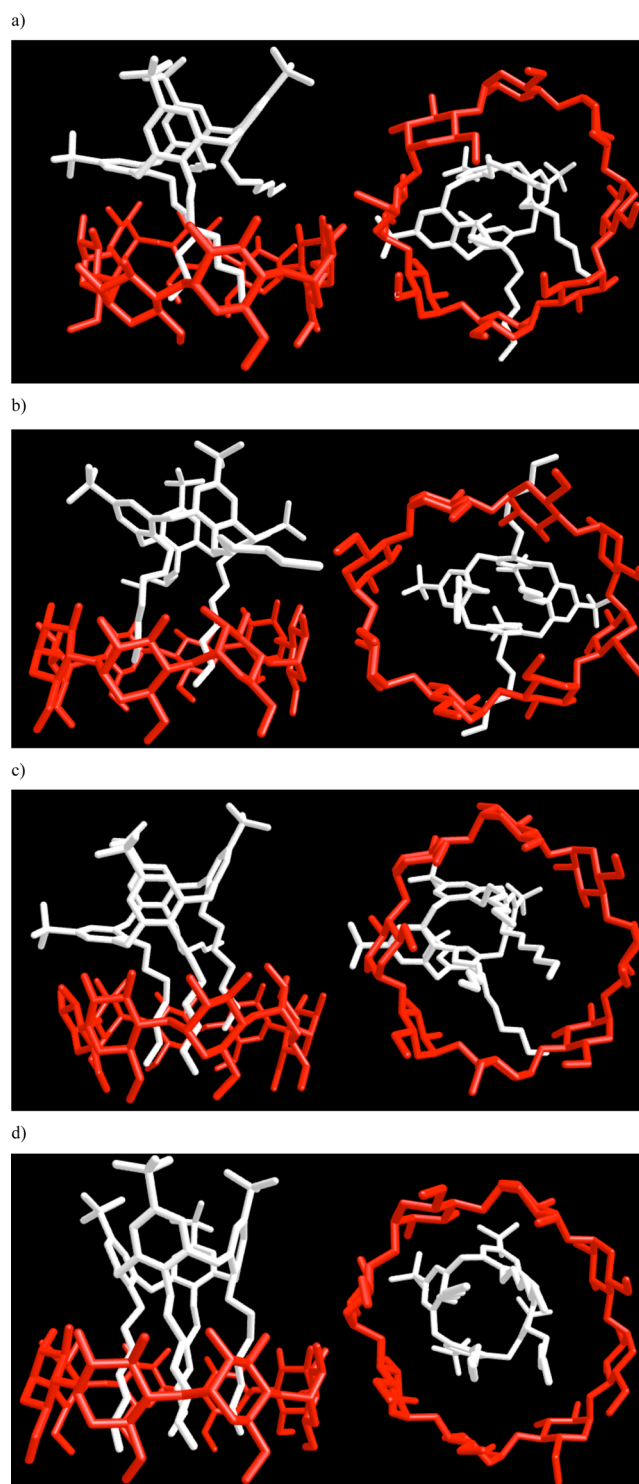


**Figure 7.** Side and bottom view of some energy-minimized structures for the complex formed between  $\gamma$ -CD (red) and SC4TH (white). Hydrogen atoms are omitted for clarity: (a) possible structure where two contiguous alkyl chains are inserted into the  $\gamma$ -CD cavity; (b) inclusion of two opposite alkyl chains; (c and d) inclusion of three and four alkyl chains, respectively.

for closed self-assembling capsules it was recently applied to macrocyclic hosts with open cavities.<sup>46</sup> Obviously, one can argue that if the alkyl chains are not fully immersed the PC can fall down near optimal values, but as rough approximation this can be used to rule out this structure. Moreover, the CD

cavities are known to present a minimum internal diameter at the altitude of the hydrogens H<sup>5</sup> and in that region the PC, for a hypothetical horizontal cross section, should be even higher.

The incorporation of three alkyl chains (Figure 7c) leads to a PC value of 0.78, while in the case where two alkyl chains (Figure 7a and b) are included the PC fall to a 0.52 optimal value. According to PC values the inclusion of two alkyl chains seems to be more likely and is supported by the fact that  $\gamma$ -CD 1:2 host-guest complexes with single-chain surfactants are frequently observed and for double chain surfactants both alkyl chains are included. However, it must be referred that the incorporation of two alkyl chains into the smaller  $\beta$ -CD cavity was suggested in an earlier work, and thus, the inclusion of more than two alkyl chains cannot be safely ruled out.<sup>47</sup>

Figure 8 shows possible structures for the 1:2 and 2:1 complexes formed between  $\gamma$ -CD and SC4TH. As mentioned

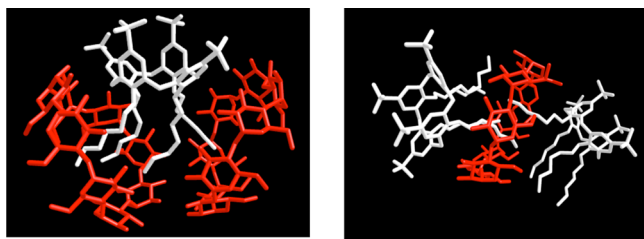


**Figure 8.** Possible structures for the (left) 2:1 and (right) 1:2 complexes formed between  $\gamma$ -CD (red) and SC4TH (white).

above, it is likely that in the 1:2 ( $\gamma$ -CD/SC4TH) complex the two calixarenes are positioned in opposite rims due to expected electrostatic repulsions and steric hindrance of placing two calixarenes in the same rim. However, as in the 1:1 complex, the number of alkyl chains that are inserted in the cavity of the  $\gamma$ -CD remain unsure. Attending to the magnitude of the binding constant  $K_2$ , which are of the same order of magnitude of  $K_1$ , and to the arguments based on the PC, it is likely that a similar number of CH<sub>2</sub> group are placed in the cavity of  $\gamma$ -CD in both 1:1 and 1:2 complexes. Along the same line, the stepwise binding constant for the formation of the 2:1 complex ( $K_3 = 20 \text{ M}^{-1}$ ), only detected for SC4TH, suggests that the second molecule of  $\gamma$ -CD interacts only with one alkyl chain of the calixarene.

**Ternary Complex Formation.** As we showed above, SC4TH and SC4TB can act as guests in the presence of  $\gamma$ -CD. Since calixarenes are better known for their ability to act as host molecules in the presence of organic and inorganic species, we also studied the formation of a ternary complex between  $\gamma$ -CD, SC4TB, and tetramethylammonium chloride (TMA). This cation was chosen because it was already demonstrated that it is complexed by SC4TB and it do not interacts with CD.<sup>48,49</sup> Thus, it seems to be the ideal guest to demonstrate the formation of the ternary complex and to investigate if the binding ability of SC4TB toward organic cations is altered when it is complexed by  $\gamma$ -CD.

The binding constant ( $K_{\text{TMA}}$ ) for the complex SC4TB/TMA was obtained by <sup>1</sup>H NMR titration experiments. In this case,

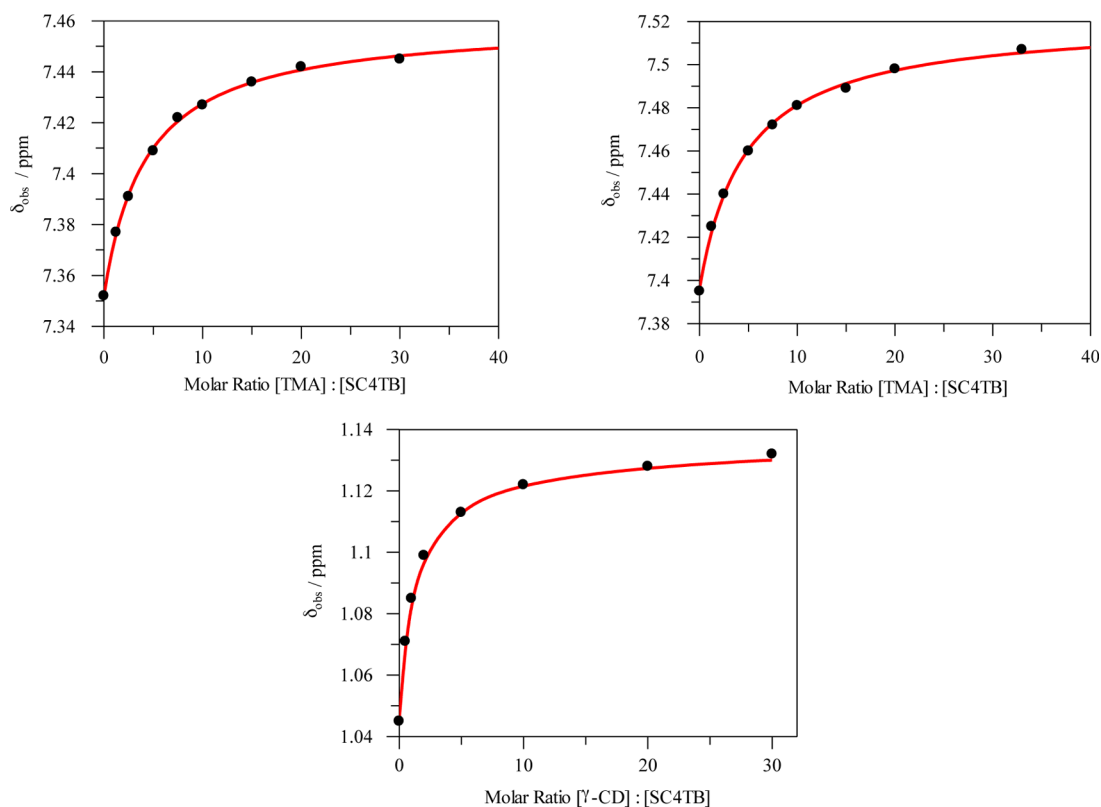
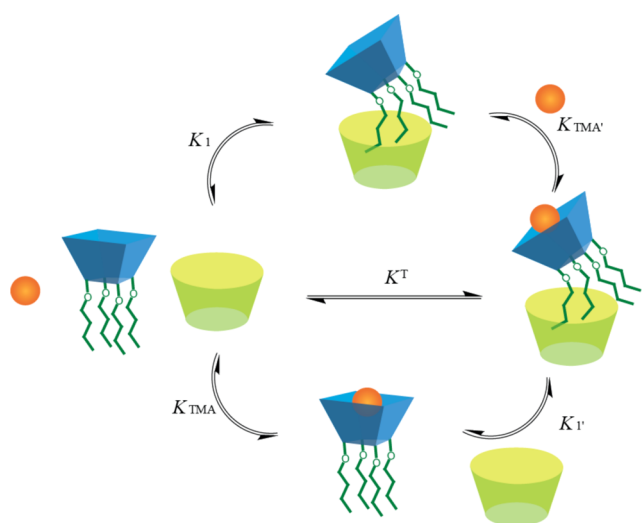


**Figure 9.** Observed <sup>1</sup>H NMR chemical shifts ( $\delta_{\text{obs}}$ ) for the Ar protons of SC4TB in the absence (left, [SC4TB] = 1 mM) and in the presence of 20 mM  $\gamma$ -CD (right, [SC4TB] = 1 mM) as a function of the [TMA]/[SC4TB] molar ratio. (Bottom)  $\delta_{\text{obs}}$  for the z protons of SC4TB (1 mM) represented against the [ $\gamma$ -CD]/[SC4TB] molar ratio in the presence of 20 mM TMA. All <sup>1</sup>H NMR experiments were carried out at 25 °C in D<sub>2</sub>O. The solid red lines of upper graphics represented the best nonlinear fit to a 1:1 binding model and the line of the bottom graph was obtained by fixing  $K_1 = 1700 \text{ M}^{-1}$  and  $K_2 = 1290 \text{ M}^{-1}$  and optimizing the chemical shifts of the z protons in the 1:1 and 1:2 complexes ( $\delta_{1,1}$  and  $\delta_{1,2}$ ).  $\delta_{1,1} = 0.089 \text{ ppm}$  and  $\delta_{1,2} = 0.034 \text{ ppm}$ .

the concentration of SC4TB was maintained constant and below the  $\text{cmc}$ ,<sup>25</sup> and the concentration of TMA was increased between 0 and 30 mM. Careful observation of the  $^1\text{H}$  NMR signals of SC4TB indicated that TMA do not induce the aggregation of the amphiphilic calixarene at the experimental conditions.<sup>25</sup> Figure 9 (upper left) shows the variation of the  $^1\text{H}$  NMR chemical shifts of the aromatic protons of SC4TB with the concentration of TMA. Fitting this data to a 1:1 binding model, a  $K_{\text{TMA}}$  value of  $280 \pm 10 \text{ M}^{-1}$  was determined. This value is compatible with that obtained in a previous work.<sup>48</sup> The experiment was repeated in the presence of 20 mM of  $\gamma$ -CD, where virtually all SC4TB is associated to the  $\gamma$ -CD as a 1:1 complex, and a value of  $K_{\text{TMA}}' = 260 \pm 18 \text{ M}^{-1}$  was obtained, indicating the formation of a ternary complex comprising SC4TB,  $\gamma$ -CD and TMA (Scheme 3). The

Scheme 3



complexation of SC4TB with  $\gamma$ -CD was also studied in the presence of 20 mM TMA, in order to ensure that most of the SC4TB molecules are associated with TMA, and it was found that the binding isotherm is not affected by the presence of the cation. As can be observed the  $\delta_{\text{obs}}$  can be perfectly described using the same parameters used to simulate the  $\delta_{\text{obs}}$  in absence of TMA (see Figure S4, Supporting Information). These results indicate that both the formation of 1:1 and 1:2  $\gamma$ -CD/SC4TB complexes is not affected by the association of SC4TB with TMA and vice versa. Conversely, the recognition site of the calixarene for small organic cations (i.e., the cavity) is not affected when it is complexed with the  $\gamma$ -CD and that the complexation of SC4TB by the CD is independent of the state of the cavity. In other words, SC4TB presents two independent binding sites.

The binding ability of SC4TB to TMA is up to 3 orders of magnitude lower than that observed for *p*-sulfonatocalix[4]arene (SC4, the nonalkylated precursor of SC4TB and SC4TH).<sup>48</sup> This is essentially due to the lower  $\pi$ -electron density and to the tighter cavity of SC4TB. The crystal structure of SC4TB suggests that this calixarene adopts a pinched cone conformation of  $C_{2v}$  symmetry in contrast with SC4 that adopts a symmetrical  $C_{4v}$  conformation that allows the guests to penetrate more deeply inside the cavity and thus maximizing the non covalent interactions established inside. Considering these arguments, the results obtained suggest that

the  $C_{2v}$  symmetry of SC4TB is maintained upon complexation with  $\gamma$ -CD. This supports the fact that the complex with four alkyl chains in the cavity is not formed because in this case SC4TB is forced to change to the  $C_{4v}$  conformation (see Figure 7d). Considering this possibility, one can expect the binding affinity of SC4TB to the TMA cation to be different, and this is not observed.

## CONCLUSIONS

In this work, we demonstrate that O-alkylated *p*-sulfonatocalix[4]arenes form 1:1, 1:2, and 2:1 host guest complexes with  $\gamma$ -cyclodextrin. While it is evident that the cyclodextrin binds the calixarenes through the hydrophobic alkyl chains, the number of alkyl chains that are incorporated in the cyclodextrin cavity for given complex remains unclear. However, the results suggest that for the 1:1 and 1:2 complexes more than one alkyl chain is incorporated into the cavity of the cyclodextrin. Although it acts as a guest in the presence of cyclodextrin, the host properties of the calixarenes remain active after the formation of the complex. This allows the formation of a ternary 1:1:1 complex with appropriate guest molecules that recognizes selectively the calixarene cavity. Tetramethylammonium chloride was shown to be a suitable molecule for the formation of such ternary complex. Finally, it was also shown that the free calixarene and the binary complex have the same affinity for the small cationic guest, indicating that the recognition abilities of the calixarene are unaffected by its inclusion in the cyclodextrin cavity.

## EXPERIMENTAL SECTION

$\gamma$ -Cyclodextrin and tetramethylammonium chloride are commercial available reagents and were used as received. The amphiphilic calix[4]arenes were available from our previous work.<sup>25</sup>  $^1\text{H}$  NMR spectra were recorded in a 300 MHz NMR instrument while DOSY experiments and ROESY were obtained in 400 and 500 MHz spectrometers, respectively. All solutions used in the NMR experiments were prepared in  $\text{D}_2\text{O}$  (99.9%). The DOSY spectra were acquired with the standard stimulated echo pulse sequence using LED and bipolar gradient pulses.<sup>50</sup> Rectangular-shaped pulse field gradients of duration 2 ms were applied with a power level linearly incremented from 2.1 to  $64.3 \text{ G cm}^{-1}$  in 20 steps. The gradient power was previously calibrated with the same DOSY experiment with a reference sample of 99%  $\text{D}_2\text{O}$  at  $25^\circ\text{C}$  ( $D = 1.872 \times 10^{-9} \text{ m}^2 \text{ s}^{-1}$ ). To obtain reliable results of the diffusion coefficient, the diffusion time  $\Delta$  of the experiment was optimized for each sample in order to capture smoothly the attenuation of the signal intensity, while affording the maximum difference in intensity between the traces with the maximum and minimum gradient power.

The microcalorimetric titrations were performed on an isothermal titration microcalorimeter at atmospheric pressure and  $25^\circ\text{C}$ . In each run, a solution of  $\gamma$ -CD in a 0.270 mL syringe was sequentially injected with stirring at 459 rpm into a solution of calixarene in the sample cell (1.459 mL volume). Each solution was degassed and thermostatted before titration. In each titration, the reference cell was filled with the same sample as that in the sample cell. The manufacturer software was used to compute the binding constants from a single titration curve with a standard deviation based on the scatter of the data points in the titration curve. The net reaction heat in each run was calculated by the "one set of binding sites" or "sequential binding sites" models. Additionally, the first point was removed from the titration curve before doing the curve-fit because of the probable leakage resulting from having the syringe stirring for a long time in the cell before the first injection, giving a smaller heat effect than it should have.



## ■ ASSOCIATED CONTENT

## ● Supporting Information

Microcalorimetric titrations fitted to a 1:1 binding model, <sup>1</sup>H NMR titrations, and Job's plot for SC4TH and SC4TB, binding models used to simulated the titration and Job's plot NMR data. This material is available free of charge via the Internet at <http://pubs.acs.org>.

## ■ AUTHOR INFORMATION

## Corresponding Author

\*E-mail: [luis.garcia@usc.es](mailto:luis.garcia@usc.es).

## Notes

The authors declare no competing financial interest.

## ■ ACKNOWLEDGMENTS

This work was supported by the Ministerio de Ciencia y Tecnología (Project No. CTQ2011-22436) and Xunta de Galicia (PGDIT10-PXIB209113PR and 2007/085). V.F. and N.B. acknowledge FCT (Portugal) for Ph.D. grants SFRH/BD/43836/2008 and SFRH/BD/29218/2006.

## ■ REFERENCES

- (1) Szejtli, J. *Chem. Rev.* **1998**, *98*, 1743–1754.
- (2) Ikeda, A.; Shinkai, S. *Chem. Rev.* **1997**, *97*, 1713–1734.
- (3) Lagona, J.; Mukhopadhyay, P.; Chakrabarti, S.; Isaacs, L. *Angew. Chem., Int. Ed.* **2005**, *44*, 4844–4870.
- (4) Biro, S. M.; Rebek, J. *Chem. Soc. Rev.* **2007**, *36*, 93–104.
- (5) Rebek, J. *Acc. Chem. Res.* **2009**, *42*, 1660–1668.
- (6) Bakirci, H.; Koner, A. L.; Schwarzlose, T.; Nau, W. M. *Chem.—Eur. J.* **2006**, *12*, 4799–4807.
- (7) Pluth, M. D.; Bergman, R. G.; Raymond, K. N. *Science* **2007**, *316*, 85–88.
- (8) Berbeci, L. S.; Wang, W.; Kaifer, A. E. *Org. Lett.* **2008**, *10*, 3721–3724.
- (9) Basilio, N.; García-Río, L.; Moreira, J. A.; Pessêgo, M. J. *Org. Chem.* **2010**, *75*, 848–855.
- (10) Harada, A.; Li, J.; Kamachi, M. *Nature* **1994**, *370*, 126–128.
- (11) Trembleau, L.; Rebek, J. *Science* **2003**, *301*, 1219–1220.
- (12) Dsouza, R. N.; Pischel, U.; Nau, W. M. *Chem. Rev.* **2011**, *111*, 7941–7980.
- (13) Jiang, L.; Yan, Y.; Huang, J. *Adv. Colloid Interface Sci.* **2011**, *169*, 13–25.
- (14) Zhang, X.; Wang, C. *Chem. Soc. Rev.* **2011**, *40*, 94–101.
- (15) Gadde, S.; Batchelor, E. K.; Weiss, J. P.; Ling, Y.; Kaifer, A. E. *J. Am. Chem. Soc.* **2008**, *130*, 17114–17119.
- (16) Dorrego, A.; García-Río, L.; Hervés, P.; Leis, J. R.; Mejuto, J.; Pérez-Juste, J. *Angew. Chem., Int. Ed.* **2000**, *39*, 2945–2948.
- (17) Nicolle, G. M.; Merbach, A. E. *Chem. Commun.* **2004**, *1*, 854–855.
- (18) Cepeda, M.; Daviña, R.; García-Río, L.; Parajó, M. *Chem. Phys. Lett.* **2010**, *499*, 70–74.
- (19) Michels, J. J.; Huskens, J.; Engbersen, J. F. J.; Reinhoudt, D. N. *Langmuir* **2000**, *16*, 4864–4870.
- (20) Dalgarno, S. J.; Atwood, J. L.; Raston, C. L. *Chem. Commun.* **2006**, 4567–4574.
- (21) Kim, S.-Y.; Jung, I.-S.; Lee, E.; Kim, J.; Sakamoto, S.; Yamaguchi, K.; Kim, K. *Angew. Chem., Int. Ed.* **2001**, *40*, 2119–2121.
- (22) Liu, S.; Zavalij, P. Y.; Isaacs, L. *J. Am. Chem. Soc.* **2005**, *127*, 16798–16799.
- (23) Liu, S.; Shukla, A. D.; Gadde, S.; Wagner, B. D.; Kaifer, A. E.; Isaacs, L. *Angew. Chem., Int. Ed.* **2008**, *47*, 2657–2660.
- (24) Guo, D.-S.; Wang, K.; Liu, Y. *J. Inclusion Phenom. Macrocycl. Chem.* **2008**, *62*, 1–21.
- (25) Basilio, N.; Garcia-Rio, L.; Martín-Pastor, M. *Langmuir* **2012**, *28*, 2404–2414.
- (26) Basilio, N.; García-Río, L.; Martín-Pastor, M. *J. Phys. Chem. B* **2010**, *114*, 4816–4820.
- (27) Shinkai, S.; Arimura, T.; Araki, K.; Kawabata, H.; Satoh, H.; Tsubaki, T.; Manabe, O.; Sunamoto, J. *J. Chem. Soc., Perkin Trans. 1* **1989**, 2039–2045.
- (28) Basilio, N.; Garcia-Rio, L. *ChemPhysChem* **2012**, *13*, 2368–2376.
- (29) Thordarson, P. *Chem. Soc. Rev.* **2011**, *40*, 1305–1323.
- (30) Cohen, Y.; Avram, L.; Frish, L. *Angew. Chem., Int. Ed.* **2005**, *44*, 520–554.
- (31) Rekharsky, M. V.; Inoue, Y. *Chem. Rev.* **1998**, *98*, 1875–1918.
- (32) Brocos, P.; Banquy, X.; Díaz-Vergara, N.; Pérez-Casas, S.; Piñeiro, A.; Costas, M. *J. Phys. Chem. B* **2011**, *115*, 14381–14396.
- (33) Tominaga, T.; Hachisu, D.; Kamado, M. *Langmuir* **1994**, *10*, 4676–4680.
- (34) Piñeiro, A.; Banquy, X.; Pérez-Casas, S.; Tovar, E.; García, A.; Villa, A.; Amigo, A.; Mark, A. E.; Costas, M. *J. Phys. Chem. B* **2007**, *111*, 4383–92.
- (35) Guerrero-Martínez, A.; Palafox, M.; Tardajos, G. *Chem. Phys. Lett.* **2006**, *432*, 486–490.
- (36) Funasaki, N.; Ishikawa, S.; Neya, S. *J. Phys. Chem. B* **2004**, *108*, 9593–9598.
- (37) Tominaga, T.; Hachisu, D.; Kamado, M. *Langmuir* **1994**, *10*, 4676–4680.
- (38) Yang, L.; Takisawa, N.; Kaikawa, T.; Shirahama, K. *Colloid Polym. Sci.* **1997**, *275*, 486–492.
- (39) De Lisi, R.; Lazzara, G.; Milioto, S.; Muratore, N. *J. Phys. Chem. B* **2003**, *107*, 13150–13157.
- (40) Ishikawa, S.; Neya, S.; Funasaki, N. *J. Phys. Chem. B* **1998**, *102*, 2502–2510.
- (41) Funasaki, N.; Neya, S. *Langmuir* **2000**, *16*, 5343–5346.
- (42) Müller, A.; Wenz, G. *Chem.—Eur. J.* **2007**, *13*, 2218–2223.
- (43) Pedretti, A.; Villa, L.; Vistoli, G. *J. Comput.-Aided Mol. Des.* **2004**, *18*, 167–173.
- (44) Zhao, Y. H.; Abraham, M. H.; Zissimos, A. M. *J. Org. Chem.* **2003**, *68*, 7368–7373.
- (45) Mecozzi, S.; Rebek, J., Jr. *Chem.—Eur. J.* **1998**, *4*, 1016–1022.
- (46) Nau, W. M.; Florea, M.; Assaf, K. I. *Isr. J. Chem.* **2011**, *51*, 559–577.
- (47) Funasaki, N.; Ishikawa, S.; Neya, S. *Langmuir* **2002**, *18*, 1786–1790.
- (48) Cui, J.; Uzunova, V. D.; Guo, D.-S.; Wang, K.; Nau, W. M.; Liu, Y. *Eur. J. Org. Chem.* **2010**, 1704–1710.
- (49) Ahmed, J.; Yamamoto, T. *J. Inclusion Phenom. Macrocycl. Chem.* **2000**, *38*, 267–276.
- (50) Wu, D.; Chen, A.; Johnson, C. S. *J. Magn. Reson., Ser. A* **1995**, *115*, 260–264.